PERGAMON

International Journal of Heat and Mass Transfer 41 (1998) 3807–3815

International Journal of
HEAT and MASS TRANSFER

Dynamic void fraction measurements in horizontal ducts with sudden area contraction

M. Fossa*, G. Guglielmini

Ditec, Dipartimento di Termoenergetica e Condizionamento Ambientale, Università degli Studi di Genova, Via Opera Pia 15a, 16145 Genova, Italy

Received 26 November 1997; in final form 25 February 1998

Abstract

Void fraction distributions in horizontal pipes with sudden area contraction have been experimentally investigated. The experiments are aimed at analysing the effect of the singularity characteristics on void fraction profiles and phase distribution. The technique employed to obtain the cross-sectional average void fraction along the test pipes is based on the instantaneous measurement of the electrical impedance of the air–water mixture. The instrumentation set up consists of ring electrode pairs placed on the internal wall of the cylindrical test duct, flush to the pipe surface. Two different test sections, a 70/60 mm i.d. pipe and a 70/36 mm i.d. pipe have been employed. Plug and slug flow regimes were investigated in order to obtain the mean void fraction along the channel in five different locations upstream and downstream the singularity. The analysis of the results, in terms of mean values and probability distributions, shows that the characteristics of the flow restriction deeply modify the flow structure upstream and downstream the discontinuity. © 1998 Elsevier Science Ltd. All rights reserved.

Key words: Void fraction measurements; Slug flow; Impedance probe; Flow in singularities

Nomenclature

D pipe diameter
D_e electrode spacing
$\dot{m}$ mass flow rate
p pressure
s electrode width
U_s superficial velocity
x distance from the contraction, also mass quality
x_v gas fraction of volume flow.

Greek symbols

α void fraction
ρ density
σ area contraction ratio.

Subscripts

g gas
l liquid.

* Corresponding author. Tel.: 00 39 10 3532198; fax: 00 39 10 311870; e-mail: mfossa@ditec.unige.it

1. Introduction

The flow of two-phase mixtures is a common situation in industrial plants such as chemical reactors, power generation units, oil wells and pipelines. As it is well known, the flow configuration and the gas–liquid interactions in such systems are a complex function of the flow rates of the two phases, of their physical properties and of pipe geometry [1, 2].

The flow structure analysis is very important to understand the basic two-phase behaviour and develop (or test) momentum and heat transfer models. In particular, considerable efforts are still being devoted to the evaluation of pressure losses in straight pipes and singularities.

0017–9310/98 $19.00
PII: S0017–9310(98)00111–2

Several models have been developed to predict the pressure drop associated with geometrical singularities, often requiring some knowledge about the phase distribution along the test channel [3–5].

A fundamental quantity, that allows the flow structure to be described quite efficiently, is the local void fraction, which can be represented either in terms of time persistence of the gas phase or, with reference to a meaningful control volume, in terms of the volume fraction occupied by the gas phase [6–8].

The knowledge of the space-time void fraction characteristics is even more important for studying the effects caused by pipe obstructions on the phase distribution along the flow channel. Unfortunately, few void fraction data are available in literature due to the difficulties related to void fraction measurements and they usually refer to straight pipes. The effects of pipe obstructions have been investigated by Salcudean et al. [9] and more recently by Arosio et al. [10]. Nevertheless, the void fraction data available refer to time averages, and providing only partial information on the actual structure of the flow.

The work presented here is an attempt to gain a deeper insight of the air–water structure in horizontal pipes when a sharp area contraction is present. The experimental observations regard the cross-sectional average void fraction evaluation in different locations along the test channel. This work is part of a program aimed at evaluating the two-phase pressure drop across sudden contractions in horizontal pipes; the operating conditions investigated cover the stratified, plug and slug flow regimes. Through the analysis of the flow structure, the study is expected also to provide an interpretation of some aspects of the two-phase interactions. In particular, the attention is focused on the peculiar trend exhibited by the singular pressure drop as a function of the gas fraction of the volume flow [2, 10, 11].

The measurements reported here are based on the impedance method [12–15]. The technique makes use of an electronic device able to measure the two-phase medium electrical conductance picked up by a pair of ring electrodes flush mounted to the pipe internal wall. With respect to other techniques, the impedance method is cost effective and allows great time savings to produce cross-sectional void data. The probes were calibrated with reference to the stratified and bubble flow configuration; some comparison with optical fibre void fraction measurements confirmed the reliability of the instrumentation adopted.

The test section is a 12 m long pipe, having a 7 m upstream part with an inner diameter D of 70 mm and a downstream part with an inner diameter of 60 or 36 mm. The tests were performed for different liquid mass flow rates (2.6, 3.2, 3.7, 4.3 kg s^{-1}) and different gas fractions of volume flows (range from 0.2–0.8). Plug and slug flow regimes were observed. Void fraction probes are five in number, two of which fit out the upstream pipe. The statistical analysis of the data records allowed the time-average void fraction and the void probability density function (PDF) to be inferred.

The analysis of the collected data, in terms of statistical indicators (mean values and PDFs), shows that the characteristics of the flow restriction deeply modify the flow structure upstream and downstream the discontinuity.

2. Impedance void meter testing and calibration

A quite common technique to study the form and the extension of the phase interface consists in the measurement of the electrical impedance of the gas–liquid two-phase region close to a system of electrodes. Thus, once the relationship between the electrical impedance of the medium and the phase distribution is provided, the average cross-sectional void fraction or a local property (e.g. the liquid film thickness in the annular flow regime) can be inferred, depending upon the extension of the measuring region.

Many studies have been carried out on impedance void meters: the main evidence is that the measured electrical impedance across an electrode pair immersed in a conducting liquid is essentially resistive when the frequency of the a.c. excitation signal is sufficiently high (10–100 kHz for tap water). With reference to the conductance method, Coney [16] has described the theoretical behaviour of flat electrodes wetted by a liquid layer, Hewitt [12] has presented a comprehensive review of the technique, Merilo et al. [17] have employed a system of conductive electrodes generating a rotating field. The studies reported in [18–21] concern the use and calibration of wire probes for liquid film thickness measurements. Ring electrodes were first employed by Asali et al. [22] while Andreussi et al. [13] and Tsochatzidis et al. [14] developed the theoretical bases regarding the response of this electrode configuration.

In the present work the conductance technique is applied by means of ring electrode pairs placed on the internal wall of the cylindrical test duct, flush to the pipe surface. An a.c. carrier voltage of 20 kHz frequency is applied across each pair of electrodes; the frequency was checked to yield a resistive behaviour of the water by measuring both the amplitude and phase shift of the applied voltage signal. An electronic device converts the a.c. signal into a d.c. signal proportional to the impedance of the two-phase medium bounded in the measuring volume defined by the two rings. The technique is similar to those adopted by other researchers and allows the average cross-sectional void fraction to be inferred, once the relationship between the medium electrical impedance and the phase distribution is provided.

The calibration curve has been obtained by means of the procedures described in [23]. The assumption adopted here concerns the possibility to describe the structure of intermittent horizontal flows as if it were constituted of stratified regions separated by liquid regions at low void fraction (slugs). The slug is here considered as a liquid domain where some bubbles can be present.

Figure 1 shows the results of the calibration procedure in terms of dimensionless conductance (the ratio between the two-phase conductance and liquid conductance). The data refer to the stratified and bubble flow configuration and different ring diameters. The electrode spacing D_e and the ring width s have been selected in order to have small measuring volumes if compared to holdup spatial fluctuations: thus the probe aspect ratios D_e/D and s/D have been chosen equal to 0.34 and 0.071, respectively. It is worthwhile to note that the fitting curve of the experimental data is in good agreement with the theoretical solution proposed by Andreussi [13].

In order to avoid continuous checking of the electrical conductivity of the liquid during operations, the measured two-phase conductance was always normalised with respect to the conductance of the full-of-liquid test pipe, and then converted into void fraction data by means of the calibration curve.

The reliability of the measuring technique has been confirmed by a comparison with single fibre optical probe data obtained at 'Politecnico' of Milano [10], where the experiments pertain to a test section with an area contraction ratio $\sigma = 0.56$ and a 60 mm i.d. downstream pipe. The impedance probe measurements concern a 70/60 mm test pipe ($\sigma = 0.73$). Figure 2 shows the cross-sectional average void fraction as a function of the gas fraction of volume flow x_v. Both data sets refer to the downstream region of the test pipe ($D = 60$ mm), respectively, 48 diameters (optical probe) and 60 diameters (impedance probe) from the contraction. The agreement between the different data sets is good, especially in the range of gas fractions from 0.3–0.6. For x_v values higher than 0.6, the optical probe data shift from the linear profile; this behaviour is probably due to the stronger area ratio, as the analysis (reported below) of the data collected with the 70/36 mm test section seems to confirm.

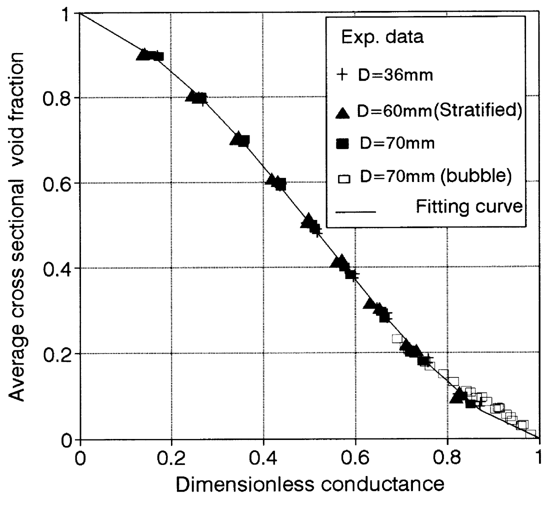

Fig. 1. Calibration curve of the ring electrode probe. Stratified (filled symbols) and bubble (open symbols) flow configurations.

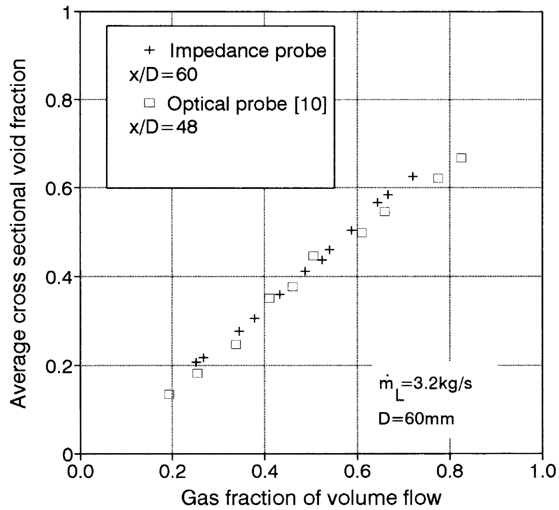

Fig. 2. Measured void fraction according different techniques. Downstream pipe ($D = 60$ mm).

3. Experimental facility and procedures

The experimental apparatus set up at Ditec, University of Genova, consists of a horizontal test section where air and water can be mixed to generate the two-phase flow under bubble, stratified and intermittent flow regimes. A complete description of the plant and procedures is available in [11]. Transparent pipes allow the inspection of the flow pattern. The test section is a 12 m long pipe with a sudden contraction of the flow area: the 7 m long upstream pipe has an inner diameter of 70 mm while the downstream pipe has an inner diameter of 60 mm (area ratio $\sigma = 0.73$) or 36 mm ($\sigma = 0.26$). The tests were performed for different liquid mass flow rates ($\dot{m}_l = 2.6$, 3.2, 3.7, 4.3 kg s^{-1}) and different gas fractions of volume flow (range from 0.2–0.8); the gas and liquid superficial velocities were thus found to be in the ranges $U_{gs} = 0.2$–6 m s^{-1} and $U_{ls} = 0.7$–2.5 m s^{-1}, respectively.

The test facility is equipped with five resistive probes, two of which are mounted upstream the discontinuity (at 8 and 15 diameters from it, respectively), while the remaining three are mounted at 4, 30 and 60 diameters downstream (60 mm pipe). The probes that fit out the 36 mm i.d. pipe are located, respectively, at 7, 30 and 70 diameters downstream from the contraction and 6, 15 diameters upstream.

The signal from each probe was picked up by the acquisition system at a sampling frequency of 200 Hz during a sampling period of at least 40 seconds. A repeatability investigation was performed over 50 test runs and at different probe locations: the standard deviation of the void fraction measurements was found to be 1.5%. The statistical analysis of the data records allowed the time-average void fraction and the void probability density to be inferred. The probability density profiles were finally employed to identify the flow pattern [24] and determine the flow conditions at which the transition from plug to slug regime occurs.

The test pipe is also equipped with fifteen pressure taps to measure the pressure profiles along the upstream and downstream pipes. The measurement of the pressure profiles allows the singular pressure drop to be extrapolated according to a typical method employed in single-phase flow studies, thus enabling the singular two-phase multiplier to be inferred by comparison with the measured liquid single-phase pressure drop.

4. Results and discussion

Some of the results related to the singular pressure drop evaluation are sketched in Fig. 3, together with the homogeneous model theoretical curve. As pointed out in previous work [2], the singular two-phase multiplier exhibits different profiles depending upon the contraction area ratios. In fact, it was observed that, for area ratios greater than 0.4, the singular multiplier did not monotonically increase with the gas fraction of volume flow at constant liquid flow rate. In particular when the area ratio is great, the two-phase multiplier shows a maximum (at x_v around 0.5) followed by a minimum. A possible explanation for this experimental evidence is the occurrence of flow pattern transitions as the flow rates increase; Fiedel and Schmidt suggested a similar explanation with reference to their own data at high gas quality [5]. The examination of the flow conditions revealed that the maximum singular pressure drop occurs roughly in correspondence with the transition between plug and slug flows, as indicated by the flow map of Mandhane et al. [29]. For low values of σ, the multiplier monotonically increases with the gas flow rate and the values are always lower than those predicted by the homogeneous model theory. From a theoretical point of view, several models have been proposed to evaluate the singular pressure drop due to a sudden contraction in the flow area [2]. Complex correlations, such as those reported in [4, 5] take into account the void fraction in the upstream and downstream regions of the channel. The capability of such correlations to evaluate the singular multiplier has been already discussed in [2] and the main conclusions are that no model is able to predict the particular trends evidenced by the experiments and that more information is needed about how the flow structure is modified by the singularity geometry. In this sense, the knowledge of the time average void fraction along the pipe is important. On the other hand the void fraction fluctuation analysis is a more powerful tool to characterise the local flow structure and regime. The void fraction α can be predicted according to several relationships. The correlations of Bankoff [25], Armand and Treshchev [26], and Chisholm [27] are based on experimental data while the correlation of Huq [28] is among the few ones based on theoretical considerations.

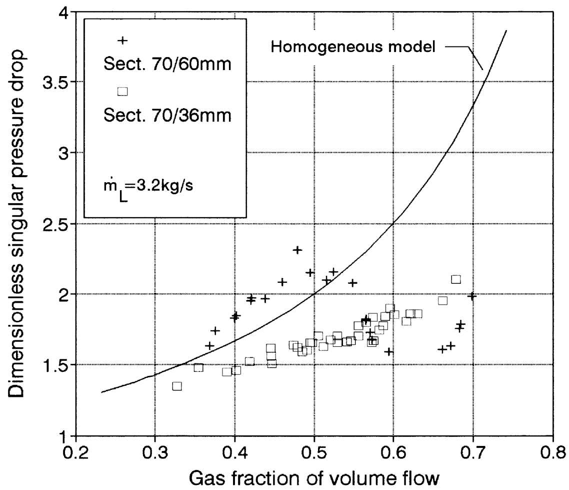

Fig. 3. Dimensionless singular pressure drop as a function of the gas fraction of volume flow for two different contraction area ratios.

In what follows, to perform some comparisons with the data presented, the Armand–Treshchev and Huq relationships have been considered; p being the pressure expressed in MPa, they, respectively, have the form:

$$\alpha = 0.833x_v + 0.05\ln(10p) \tag{1}$$

$$\alpha = 1 - \frac{2(1-x)^2}{1-2x+\sqrt{1+4x(1-x)\left(\frac{\rho_l}{\rho_g}-1\right)}}. \tag{2}$$

As an example, Figs 4(a) and (b) show two data sets collected with one of the impedance probes in terms of liquid holdup vs. time. The position of the probes is referred to an x-axis oriented in the same direction as the flow and whose origin is at the contraction. The measuring station is located on the upstream pipe, close to the singularity. Both figures refer to a 70 mm i.d. pipe under the same flow conditions, but two different restrictions are considered. The typical phase distribution of the intermittent flow (a sequence of aerated slugs and

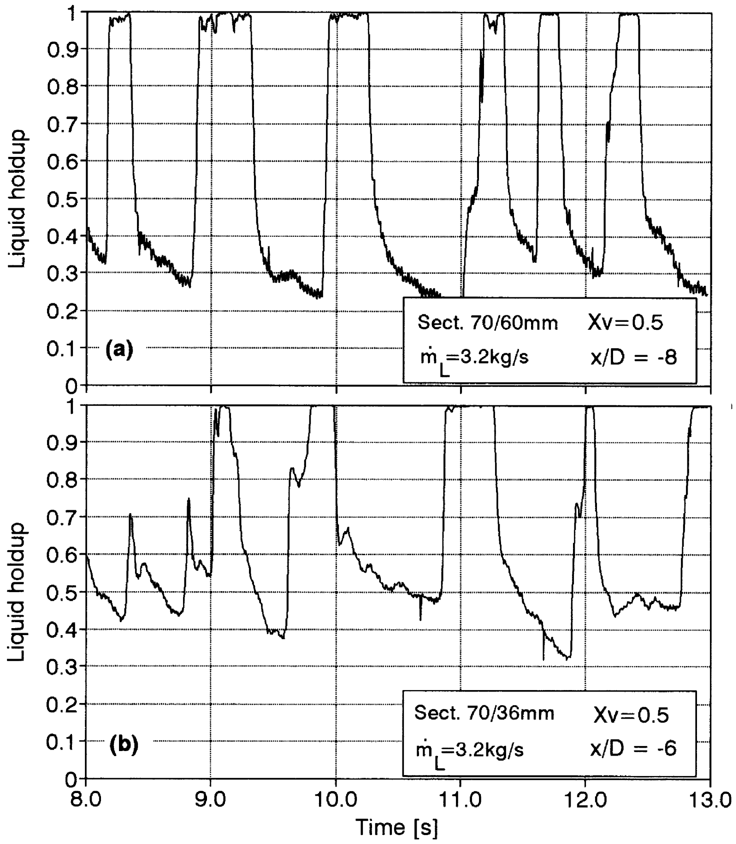

Fig. 4. Liquid holdup fluctuations in the upstream pipe close to the singularity. $D = 70$ mm, $x_v = 0.5$, $\sigma = 0.73$ (a), $\sigma = 0.26$ (b).

stratified regions) is evidenced. The effect of the geometry on the flow structure can be noticed: the stronger contraction ($\sigma = 0.26$, Fig. 4(b)) causes a more pronounced liquid deceleration and, consequently, a greater liquid holdup than produced by the contraction of area ratio 0.73. This behaviour is in agreement with the observations of Salcudean and co-workers [9] who studied the effects on the flow structure caused by a flange-type obstruction inserted within a horizontal pipe. Their experiments showed that the singularity affects the flow pattern either downstream or upstream the obstruction.

Data sets similar to those reported in Fig. 4 have been employed to evaluate the time average values of the void fraction along the test pipes. Figures 5 and 6 refer to the 70/60 mm test section ($\sigma = 0.73$) and show the void fraction variations as a function of the gas fraction of volume flow.

In Fig. 5 the average void fraction values are presented for the liquid mass flow rate of 3.2 kg s^{-1} with the distance from the contraction as a parameter. The figure shows that the void fraction does not change significantly along

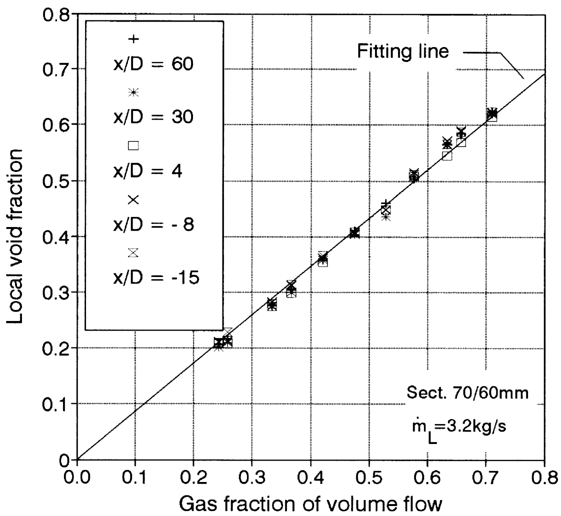

Fig. 5. Average cross-sectional void fraction as a function of the gas fraction of volume flow. Parameter: distance from the contraction. Test section 70/60 mm.

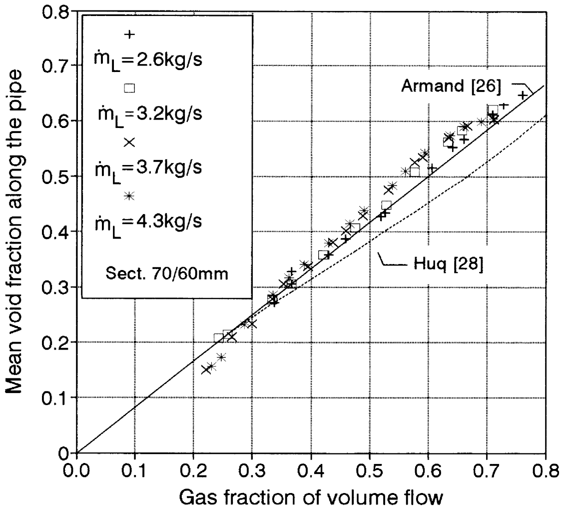

Fig. 6. Average void fraction along the pipe as a function of the gas fraction of volume flow. Parameter: liquid flow rate. Test section 70/60 mm.

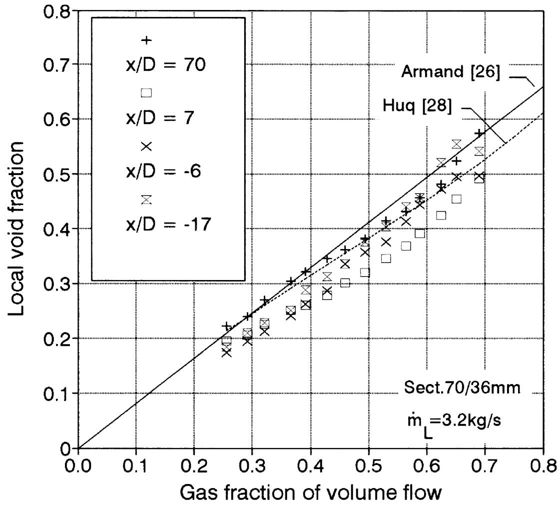

Fig. 7. Average cross-sectional void fraction as a function of the gas fraction of volume flow and the liquid flow rate. Test section 70/36 mm.

the channel (even if local variations may occur very close to the contraction where no data were collected) and that an almost linear relationship exists between α and x_v, as suggested by the correlation of Armand and Treshchev but with a slightly smaller slope. As the liquid flow rate increases, the measured gas fraction profile seems to deviate from the linear trend as depicted in Fig. 6 where the mean void fraction along the channel (averaged over five probe values) is presented as a function of x_v with the liquid flow rate as a parameter.

Figures 7 and 8 show the data collected with the 70/36 mm test section. The analysis of the void fraction profiles shows some peculiar characteristics with respect to the data collected with the 70/60 mm pipe. The differences between the two data sets mainly concern the void fraction variations along the pipe occurring when the contraction is greater. As depicted in both figures, the void fraction decreases close to the discontinuity where a minimum value is probably attained; similar trends have also been reported in [2], where an optical fibre probe was employed to collect the void data. Furthermore, in agreement with ref. [2], far from the contraction, the void fraction profile shifts from the linear profile at x_v values higher than 0.40.

The effect of the liquid flow rate with reference to the above observations does not seem to be remarkable. It is interesting to point out that the void fraction values for $\sigma = 0.26$ are always lower than those relevant to $\sigma = 0.73$, even when the measurements refer to the upstream pipe, whose diameter is the same for the two test section ($D = 70$ mm).

This finding can be illustrated in terms of probability density function of the void fraction fluctuations in time.

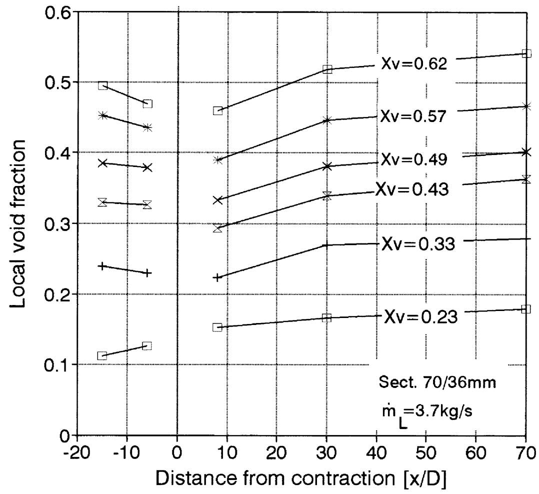

Fig. 8. Average cross-sectional void fraction as a function of the distance from the contraction for different values of x_v. Test section 70/36 mm.

As an example, Fig. 9 shows the probability density function profiles inferred from the data collected in the upstream pipe of the two test sections under the same flow conditions as reported in Fig. 4. The measuring stations are those adjacent to the obstruction, at 8 diameters ($\sigma = 0.73$) and 6 diameters ($\sigma = 0.26$) from it, respectively. The curves exhibit the typical profile relevant to the intermittent flow, characterised by two peaks: a high void fraction peak relative to the mean holdup in the stratified region between slugs and a low

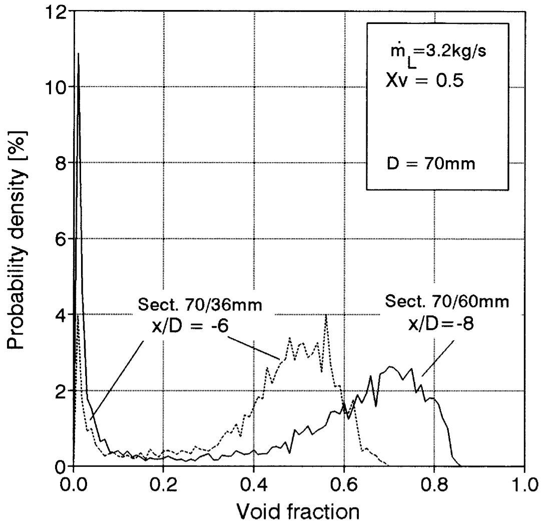

Fig. 9. Probability density functions of the void fraction records with the pipe area ratio as a parameter.

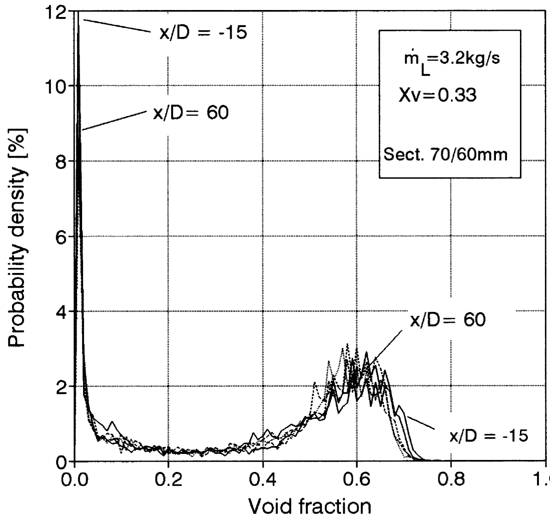

Fig. 10. Probability density functions of the void fraction records with the distance from the contraction as a parameter. Test section 70/60 mm.

void fraction peak relative to the mean slug holdup [24]. The curves in Fig. 9 differ from each other not only in mean value over time but also in shape. The height of the low void fraction peak relative to the 70/60 mm pipe may be interpreted as the occurrence of a well developed and regular intermittent flow where the presence of (almost) deaerated liquid slugs (plugs) is the main feature. On the contrary, the probability density curve relative to the stronger obstruction pipe reveals a more chaotic phase distribution where the percentage of low void fraction slugs is lower: in this situation the two peaks have similar heights and the flow regime, according to Costigan and Whalley [15], can be classified as 'stable slug' flow.

Figure 10 shows the probability density curves relative to the 70/60 mm pipe with the distance from the contraction as a parameter. Here the liquid flow rate is 3.2 kg s^{-1} ($U_{ls} = 0.83$ m s^{-1} in the downstream pipe) and $x_v = 0.33$, but similar results have been obtained with different liquid flow rates. One can observe that the flow structure remains substantially unchanged along the pipe and that the singularity seems to have little influence on the mixture characteristics: the five curves practically coincide and the low void fraction peaks exhibit a narrow range of values (9–12%). As for the effects of the gas flow rate, Fig. 11 shows the probability density curve evolution as the gas fraction of volume flow changes. The figure considers the downstream region of the 70/60 mm pipe ($xD = 60$) at $\dot{m}_l = 3.2$ kg s^{-1}. The main feature of this and other PDF diagrams pertaining to the $\sigma = 0.73$ test section at constant liquid flow rate consists in the passage from a double peak configuration to a single peak configuration as the gas flow rate increases.

It is interesting to note, that the height of low void

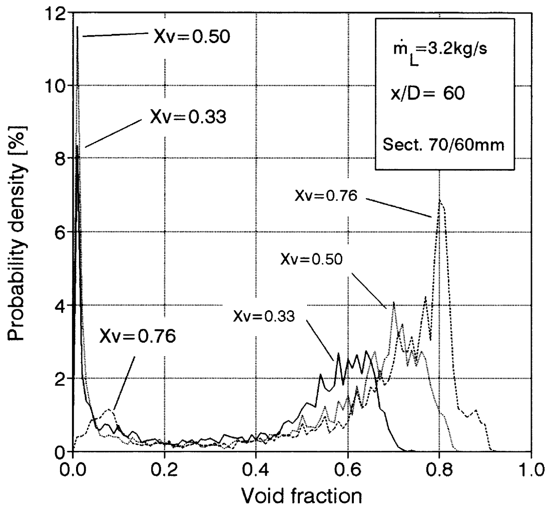

Fig. 11. Probability density functions of the void fraction records with the gas fraction of volume flow as a parameter. Test section 70/60 mm.

fraction peak (slug peak) goes through a maximum while the flow regime evolves from plug to ('stable' and then 'unstable', [15]) slug flow as an effect of the gas flow rate increase. The recognition of the flow regime transitions and of the flow regimes themselves is still a matter of discussion; indeed several names are encountered in the literature to define the two-phase flow configurations. Nevertheless, the occurrence of a maximum of the slug peak height as a function of x_v may be interpreted as the occurrence of regime transition from plug to slug flow. The transition takes place at x_v values around 0.5, the corresponding U_{gs} values being in the 0.9–1.1 m s^{-1} range. The old map of Baker [30], the Mandhane flow map and the flow map of Barnea [31] indicate this location for the transition from plug to slug flow. This fact may constitute a key to interpret the particular trend exhibited by the singular multiplier as reported in Fig. 3, thus, ascribing the non-monotonical profile of the multiplier to the occurrence of changes of the flow regime in both the upstream and downstream pipe.

The analysis of the PDFs relevant to the $\sigma = 0.26$ test section reveals a different behaviour. The shape of the PDF curve changes considerably depending upon the measuring station, as Fig. 12 illustrates. In particular, the diagram shows that the slug peak modifies its height according to the distance from the contraction at which the void data record was collected. On the contrary, the void fraction value at which the peak occurs does not seem to change ($\alpha = 0.03$): the air content in the slugs does not vary while the number of deaerated slugs does. Moreover, it is interesting to observe the PDF profile concerning the measuring station just downstream the discontinuity, where the void fraction generally reaches its minimum (measured) value along the channel. Here the slug peak is at its highest value, as if the contraction strengthened the intermittent behaviour of the flow by arranging the flow into regular alternating fluid packets, full liquid slugs and fast wavy bubbles. This fact may be correlated to the observations of Salcudean and co-workers, who concluded that the presence of a peripheral obstruction affects the local flow pattern extending the intermittent regime domain beyond the flow condition region pertinent to the smooth pipe.

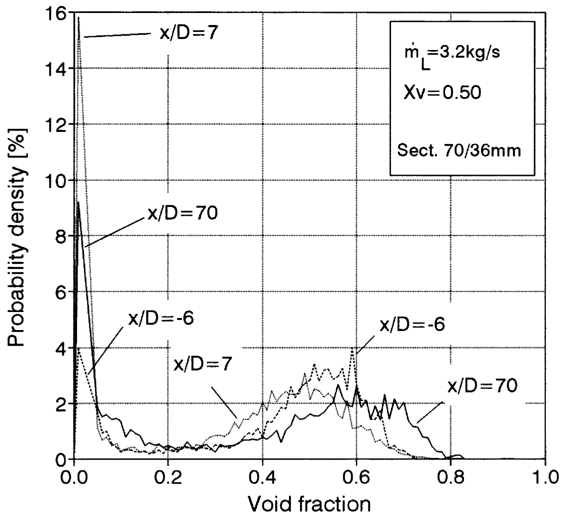

Fig. 12. Probability density functions of the void fraction records with the distance from the contraction as a parameter. Test section 70/36 mm.

The effects of the flow rates of liquid and gas on the PDF curves are similar to those observed with the $\sigma = 0.73$ test section. At constant liquid flow rate, as the value of x_v increases the intermittent structure of the flow changes into a configuration in which it is difficult to distinguish the regions with liquid predominance from those where the gas prevails.

5. Conclusions

The impedance method was adopted to measure the cross-sectional void fraction in two-phase flows developing in horizontal pipes with a sudden area contraction. The instrumentation set up, which employs closely spaced ring electrodes, was proved to be suitable for coupled local and instantaneous analysis of the two-phase flow structure. The experiments were carried out with two test sections having the same upstream pipe ($D = 70$ mm) but different area contraction ratios ($\sigma = 0.73, 0.26$). The investigated flow conditions cover the plug and slug flow regimes.

With reference to the $\sigma = 0.73$ pipe, the results obtained in terms of void fraction mean values are in good agreement with the correlation of Armand and Treshchev, and the presence of the obstruction seems to exert little influence on the void distribution along the channel. The effect of the singularity is stronger with the $\sigma = 0.26$ pipe: the void fraction values are always lower than those predicted, and minima occur at the discontinuity. The void fraction profile approaches again the Armand–Treshchev line only far from the discontinuity in the downstream region and for low values of x_v. Upstream the discontinuity the characteristics of the restriction deeply modify the phase distribution when compared to the $\sigma = 0.73$ pipe under the same flow conditions.

PDFs have been inferred from time records of the void fraction signals. The PDF profiles relevant to the $\sigma = 0.73$ test pipe slightly change with the distance from the contraction while considerable variations appeared with the $\sigma = 0.26$ test pipe, in which case the contraction seems to strengthen the intermittent structure of the flow just downstream the discontinuity.

Acknowledgement

This work was supported by Grant "Cofinanziamento MURST 1997, progetto Termofluidodinamica mono e bifase".

References

[1] Azzopardi BJ, Sudlow CA. The effect of pipe fittings on the structure of two-phase flow. Proc 11th Heat Transfer Congress UIT, Milan, 1993.

[2] Guglielmini G, Muzzio A, Sotgia G. The structure of two-phase flow in ducts with sudden contractions and its effect on the pressure drop. Proc 4th World Conf ExHTF, Brussels, June, 1997.

[3] Patrick M, Swanson BS. Expansion and contraction of an air–water mixture in vertical flow. AIChEJ 1959;5:444–5.

[4] Janssen E. Two-phase pressure loss across abrupt area contractions and expansions: steam water at 600–1400 psia. 3rd Int Heat Transfer Conf 1966;5.

[5] Schmidt J, Friedel L. Two-phase pressure drop across sudden contractions in duct areas. Int J Multiphase Flow 1997;23:283–99.

[6] Cartellier A, Achard JL. Local phase detection probes in fluid/fluid two-phase flow. Rev Sci Instrum 1991;62:279.

[7] Hetsroni G. Handbook of Multiphase System. Hemisphere, 1982.

[8] Bergles AE, Collier JG, Delhaye JM, Hewitt GF, Mayinger F. Two-Phase Flow and Heat Transfer in the Power and Process Industries. Hemisphere, 1981.

[9] Salcudean M, Chun JH, Groneveld DC. Effect of flow obstruction on void distribution in horizontal air–water flow. Int J Multiphase Flow 1983;9:91–6.

[10] Arosio S, Muzzio A, Sotgia G. Void fraction distribution during adiabatic two-phase flow in a horizontal pipe with sudden contraction. 2nd European Thermal Sciences and 14th UIT Congress, Rome, June, 1996.

[11] Guglielmini G, Soressi E. Experimental data of two-phase pressure drop across sudden area contractions in horizontal flow. Proc 5th Int Conf Multiphase Flow in Industrial Plants, Amalfi, Italy, September, 1996.

[12] Hewitt GF. Measurement of Two-Phase Parameter. Academic Press, London, 1978.

[13] Andreussi P, Di Donfrancesco A, Messia M. An impedance method for the measurement of liquid hold-up in two phase flow. Int J Multiphase Flow 1988;14:777.

[14] Tsochatzidis NA, Karapantios TD, Kostoglou MV, Karabelas AJ. A conductance method for measuring liquid fraction in pipes and packed beds. Int J Multiphase Flow 1992;5:653.

[15] Costigan G, Whalley PB. Slug flow regime identification from dynamic void fraction measurement in vertical air–water flows. Int J Multiphase Flow 1997;23:263–82.

[16] Coney MWE. The theory and application of conductance probes for the measurement of liquid film thickness in two phase flow. J Phys E: Scient Instrum 1973;6:903–10.

[17] Merilo M, Dechene RL, Cichowlas WM. Void fraction measurements with a rotating electric field conductance gauge. J Heat Transfer 1977;99:330–2.

[18] Brown RC, Andreussi P, Zanelli S. The use of wire probes for the measurement of liquid thickness in annular gas–liquid flows. Can J Chem Eng 1978;56:754–7.

[19] Karapantios TD, Paras SV, Karabelas AJ. Statistical characteristics of free falling films at high Reynolds numbers. Int J Multiphase Flow 1989;15:1–21.

[20] Koskie JE, Mudawar I, Tiederman WG. Parallel wire probes for measurements of thick liquid films. Int J Multiphase Flow 1989;15:521–30.

[21] Kang HC, Kim MH. The development of a flush wire probes and calibration method for measuring liquid film thickness. Int J Multiphase Flow 1992;18:423–37.

[22] Asali JC, Hanratty TJ, Andreussi P. Interfacial drag and film height for vertical annular flow. AIChEJ 1985;31:895–902.

[23] Fossa M. Design and performance of a conductance probe for measuring the liquid fraction in two-phase gas–liquid flows. J Flow Meas and Instr 1998.

[24] Jones OC, Zuber N. The interrelation between void fraction fluctuations and flow patterns in two-phase flow. Int J Multiphase Flow 1975;2:273–306.

[25] Bankoff SG. A variable density single fluid model for two-phase flow with particular reference to steam–water flow. ASME J Heat Transfer 1960, 265.

[26] Armand AA, Treshchev G. Investigation of the resistance during the movement of steam–water mixtures in heated pipe at high pressure. AERE Lib/Trans 1959, 81.

[27] Chisholm D. Two phase flow in pipelines and heat exchangers. G. Godwin, London, 1983.

[28] Huq R. An analytical two-phase void fraction prediction method. AIAA/ASME 5th Joint Term and Heat Transfer Conf, 1990.

[29] Mandhane JM, Gregory GA, Aziz K. A flow pattern map for gas–liquid flows in horizontal pipes. Int J Multiphase Flow 1974;1:537–53.

[30] Baker O. Simultaneous Flow of Oil and Gas 1954;53:185.

[31] Barnea D. A unified model for predicting flow-pattern transitions for the whole range of pipe inclinations. Int J Multiphase Flow 1987;13:1–12.